Chemical Engineering Journal 379 (2020) 122396

Contents lists available at ScienceDirect

Chemical Engineering Journal

journal homepage: www.elsevier.com/locate/cej

Novel hydroxyapatite-based bio-ceramic hollow fiber membrane derived from waste cow bone for textile wastewater treatment

Siti Khadijah Hubadillah[a], Mohd Hafiz Dzarfan Othman[a,*], Zhong Sheng Tai[a], Mohd Riduan Jamalludin[b], Nur Kamilah Yusuf[c], Azlan Ahmad[d], Mukhlis A. Rahman[a], Juhana Jaafar[a], Siti Hamimah Sheikh Abdul Kadir[e], Zawati Harun[f]

[a] Advanced Membrane Technology Research Centre (AMTEC), Universiti Teknologi Malaysia, 81310 Skudai, Johor, Malaysia
[b] Faculty of Engineering Technology, Universiti Malaysia Perlis (UniMAP), Kampus UniCITI Alam, Sungai Chuchuh, Padang Besar 02100, Perlis, Malaysia
[c] Sustainable Manufacturing and Recycling Technology, Advanced Membrane Technology Research Centre (SMART-AMMC), Universiti Tun Hussein Onn Malaysia, 86400 Parit Raja, Batu Pahat, Johor, Malaysia
[d] Department of Mechanical Engineering, Faculty of Engineering, Universiti Teknologi PETRONAS, 32610 Seri Iskandar, Perak, Malaysia
[e] Institute of Molecular Medicine and Biotechnology, Faculty of Medicine, Universiti Teknologi MARA Sungai Buloh Campus, Selangor Branch, Jalan Hospital, 47000 Sungai Buloh, Selangor, Malaysia
[f] Advanced Materials and Manufacturing Centre (AMMC), Faculty of Mechanical and Manufacturing Engineering, Universiti Tun Hussein Onn Malaysia, 86400 Parit Raja, Batu Pahat, Johor Darul Takzim, Malaysia

HIGHLIGHTS

- Novel ceramic membranes were derived from waste cow bone for textile wastewater.
- Membrane structure comprises of the cylindrical rod-shaped HAp particles.
- The membrane can effectively treated textile wastewater through hybrid separation-adsorption mechanism.
- High rejections of color (99.9%), COD (80.1%), turbidity (99.4%) and conductivity (30.1%) were obtained.

ARTICLE INFO

Keywords:
Ceramic membrane
Cow bone
Hydroxyapatite (HAp)
Wastewater treatment

ABSTRACT

Industrial textile wastewater is toxic due to the presence of recalcitrant color pigments and poisonous heavy metals. In this study, the hydroxyapatite (HAp)-based bio-ceramic hollow fiber membranes (h-bio-CHFM) were developed via the combined phase inversion and sintering technique. It was found that the properties of the developed h-bio-CHFMs were greatly affected by the HAp content of the ceramic suspension, and sintering temperature. The h-bio-CHFM with the sintering temperature of 1200 °C exhibited the long rod-shaped HAp particles and the smallest pore size (0.013 μm). High removals of color (99.9%), COD (80.1%), turbidity (99.4%) and conductivity (30.1%) were achieved using the h-bio-CHFM sintered at 1200 °C with stable high flux of 88.3 L/m^{2}h. Remarkably, the h-bio-CHFM sintered in the temperature range of 1000–1200 °C also demonstrated excellent adsorption ability towards heavy metals with 100% removals. The results of this study show the potential of the h-bio-CHFM for the efficient industrial textile wastewater treatment applications.

1. Introduction

The textile industry is one of the major industries in the world that hugely contribute to global pollution [1]. The wastewater emitted from the textile industry usually contains textile dyes, suspended solids, mineral oils and surfactants; and is generally high in biochemical oxygen demand (BOD) and chemical oxygen demand (COD). The dye concentration of the textile wastewater may range up to 1000 mg/L^{-1} [2]. In addition, the wastewater also consists of highly toxic heavy metals such as lead (Pb), chromium (Cr) and cadmium (Cd). These heavy metals are widely used in the production of the color pigment of textile dyes. In this regard, it could be trapped in the soil and bioaccumulate in the human body and aquatic life after discharging to the environment. Hence, numerous technologies have been introduced to

* Corresponding author.
E-mail addresses: dzarfan@utm.my, hafiz@petroleum.utm.my (M.H.D. Othman).

https://doi.org/10.1016/j.cej.2019.122396
Received 17 March 2019; Received in revised form 29 July 2019; Accepted 31 July 2019
Available online 01 August 2019
1385-8947/

treat the textile wastewater in a green, economically feasible and efficient way [3,4].

Membrane technology has been widely recognized for textile wastewater treatment. Zeng et al. successfully removed the dyes from textile wastewater using the polyvinylidene fluoride (PVDF) membranes blended with dopamine-modified halloysite nanotubes [5]. The results showed that the electronegativity and adsorption ability of the nanotubes significantly contributed to the high flux and dye removal. Arumugham et al. fabricated a novel polyphenylsulfone membrane which was able to reject > 99% of cationic dye from water [6]. However, it is known that polymeric membranes exhibit several drawbacks such as low thermal and chemical resistivity. On the other hand, ceramic membranes possess outstanding resistance to thermal and chemical attacks. Nevertheless, the fabrication of the commercial ceramic membranes, which are commonly prepared from alumina, involves high sintering temperature which makes the production cost extremely expensive. Therefore, the development of cost-effective ceramic membranes from natural materials such as clays [7–9] and waste materials [10,11] has grown inexorably in recent years. For instance, Fang et al. developed a cost-effective ceramic membrane from waste fly ash for oily-wastewater treatment application [12]. The fly ash membrane demonstrated better flux performance, lower membrane fouling resistance and higher oil removal. Lü et al. fabricated a low cost ceramic membrane from coal gangue and bauxite [13]. The membrane exhibited a unique structure composed of rod-like particles which gradually grew into blocky-like particles with increasing sintering temperatures from 1100 to 1400 °C. As a result, the mechanical strength of the membrane was enhanced. In our recent work, we successfully developed a low-cost ceramic membrane from waste rice husk ash through a combined phase inversion and sintering technique for adsorptive membrane application [14]. The main reason that rice husk ash was chosen for that study was due to the abundance of the waste rice husk ash. Apart from providing low-cost ceramic material, the utilization of waste rice husk ash could minimize the environmental and health problems arose from the open waste disposal. The rice husk ash membrane showed its potential in wastewater treatment with excellent heavy metals removal performance of up to 99.9%.

A massive 2.12 billion tons of solid waste is generated every year. Municipal solid waste (MSW) accounts for 61% of the total waste; its annual generation was reported to reach 1.3 billion ton in 2010 [15]. It is expected that the MSW generation will increase to 2.2 billion ton per year by 2025 [16]. In Malaysia, the amount of MSW has increased by more than 91% in the last decade [17]. Due to this, the Malaysian government has highlighted the MSW management as an important agenda in ensuring the successful development of the country. According to Zheng et al., most of the MSW is disposed of by landfills [18]. For example, 54% of MSW in the United States and 77% of MSW in China are dumped in the landfill. In Malaysia, kitchen waste dominated the amount of MSW found in the landfill [19]. Waste animal bones (WAB) such as cow bones, fish bones, chicken bones, pig bones, etc., are among the main types of kitchen waste. A study conducted by Shahzad et al. found that waste cow bone (WCB) was the main waste stream of the total MSW generated in Makkah city [20]. Hence, the utilization of these WAB is crucial to minimize the problems related to open disposal.

Nowadays, WAB have been widely explored as an alternative source for various applications such as biodiesel production, wastewater treatment, and medical applications. WAB contains a precious bio-ceramic material known as hydroxyapatite (HAp). HAp is a calcium phosphate with exceptional biocompatibility, osteoconductivity and osteoinductivity [21–23]. Several synthesizing routes have been introduced to produce HAp from WAB, such as precipitation [24], hydrothermal process [25], thermal treatment [26], etc. Among all these methods, thermal treatment is the most common treatment used to prepare HAp from WAB as reported in the literature. Studies have reported the use of HAp in wastewater treatment applications. For example, Lemlikchi et al. [27] successfully treated industrial textile wastewater via HAp co-precipitation. The presence of calcium and phosphate in HAp acted as the adsorbents for color and other pollutants in textile wastewater, such as heavy metals. Remarkably, the HAp precipitation occurred near neutral pH values which allowed the treated water to return to the environment without further pH adjustment. Moreno et al. investigated the feasibility of HAp derived from WCB on the removal of magnesium, iron, nickel and copper from wastewater [28]. The results showed that the HAp exhibited high adsorption capacity towards these heavy metals. In another recent study, Slimani et al. prepared HAp from WAB which was collected from a butcher shop. The WAB was cleaned, crushed and sintered at 800 °C for 2 h [29]. The compositional analysis demonstrated that the WAB was successfully converted into HAp after sintering. The obtained HAp was then used for the treatment of wastewater containing copper and zinc.

The present work reports on the fabrication of the novel hydroxyapatite-based bio-ceramic hollow fiber membrane (h-bio-CHFM) derived from WCB using combined phase inversion and sintering technique. As far as we are concerned, no ceramic membrane has been fabricated from cow bone waste. This bio-ceramic membrane can be an outstanding solution for the high cost commercial ceramic membrane. WCB was chosen in this study due to high calcium content and its ability to produce HAp in large quantity [30]. Prior to the membrane fabrication process, the WCB was converted to HAp via thermal treatment at 800 °C. The hollow fiber membrane morphology could be greatly varied by changing the HAp content and sintering temperature. The properties of h-bio-CHFMs were studied through scanning electron microscopy (SEM), mercury intrusion porosimetry (MIP) analysis and three-point bending test. The separation performance of h-bio-CHFMs was determined using industrial textile wastewater.

2. Materials and methods

2.1. Materials

The WCB were obtained from a local butcher shop in Johor, Malaysia. Polyethersulfone (PESf, Radel A-300, Ameco Performance, USA), N-methyl-2-pyroolidone (NMP, QRëC™) and Arlacel P135 (polyethyleneglycol 30-dipolyhydroxystearate, CRODA) were used as the polymer binder, solvent and dispersant, respectively. Tap water was used as the bore fluid and coagulant bath.

2.2. Preparation of hydroxyapatite powder from waste cow bones

The 10 kg of WCB were first manually crushed into smaller pieces. Next, the bones were boiled in hot water at the temperature of 100 °C to remove the attached tissues and fats. The bones were later dried in an oven at 100 °C for 24 h. After drying, the bones were crushed and calcined in a muffle furnace (Magna V) at the temperature of 800 °C for 3 h with the heating rate of 10 °C /min [26]. The temperature of the furnace was let to cool down to room temperature at 10 °C /min. After the calcination process, the calcined bones were milled into powders using a planetary ball mill. The powders were finally sieved to obtain about 8.3 kg fine HAp powder with the size of less than 36 μm. The overall powder preparation process is illustrated in Fig. 1.

2.3. Characterization of hydroxyapatite powder from waste cow bones

Transmission electron microscopy (TEM, JEOL JEM-2010, Japan) was used to study the morphology and selected area electron diffraction (SAED) pattern of HAp derived from WCB. The phase and crystallinity information of HAp was obtained using X-ray diffractometer (XRD, Rigaku, Japan) with Cu Kα radiation (λ = 1.540 Å) over the Bragg angle ranging from 10 to 60°. The spectroscopic characterization of HAp was investigated via the fourier transform infrared analysis (Varian FTS 1000 FT-IR, Mid-IR spectral range, cooled DTGS detector, Scimitar series, Varian Inc., Australia). The sample was prepared using

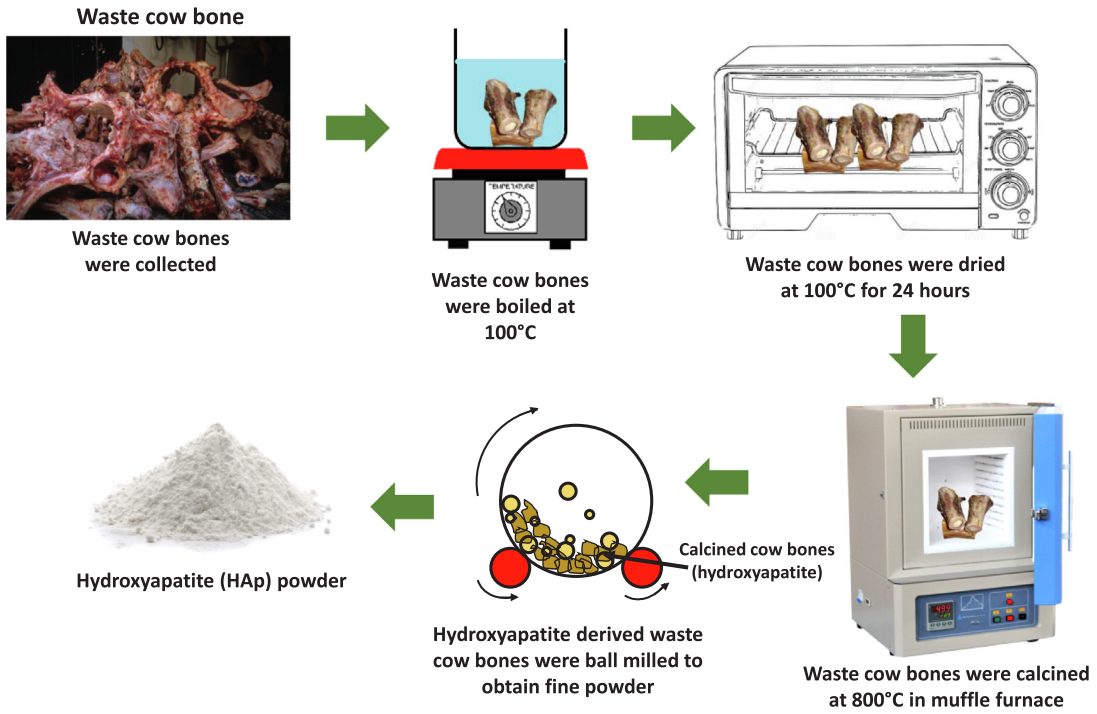

Fig. 1. Schematic diagram for the preparation of HAp derived from WCB.

the KBr pellet technique. The thermal properties of HAp were studied using the thermalgravimetric analyzer (TGA, Pyris1, Perkin Elmer Inc., USA).

2.4. Preparation of hydroxyapatite-based bio-ceramic hollow fiber membrane

Fig. 2 illustrates the preparation of h-bio-CHFMs using the combined phase inversion and sintering technique [31,32]. First, the dope suspensions with different HAp contents were prepared by dissolving the NMP as solvent, HAp and 1 wt% of Arlacel as dispersant. The HAp content of the suspensions was varied from 40 to 60 wt%. The suspension was milled for 24 h using six and two zirconia milling balls with the diameters of 6 and 12 mm, respectively. After that, 5 wt% of PESf was added to the suspension as binder which was further milled for another 48 h. The homogeneous HAp suspension was degassed under vacuum (Self-cleaning Dry Vacuum System, Model 2025, Welch) with stirring (OST 20 digital, Verisiserv) for approximately one hour. After degassing, the suspension was transferred to a 100 mL stainless steel syringe for extrusion. The flow rate of the suspension was

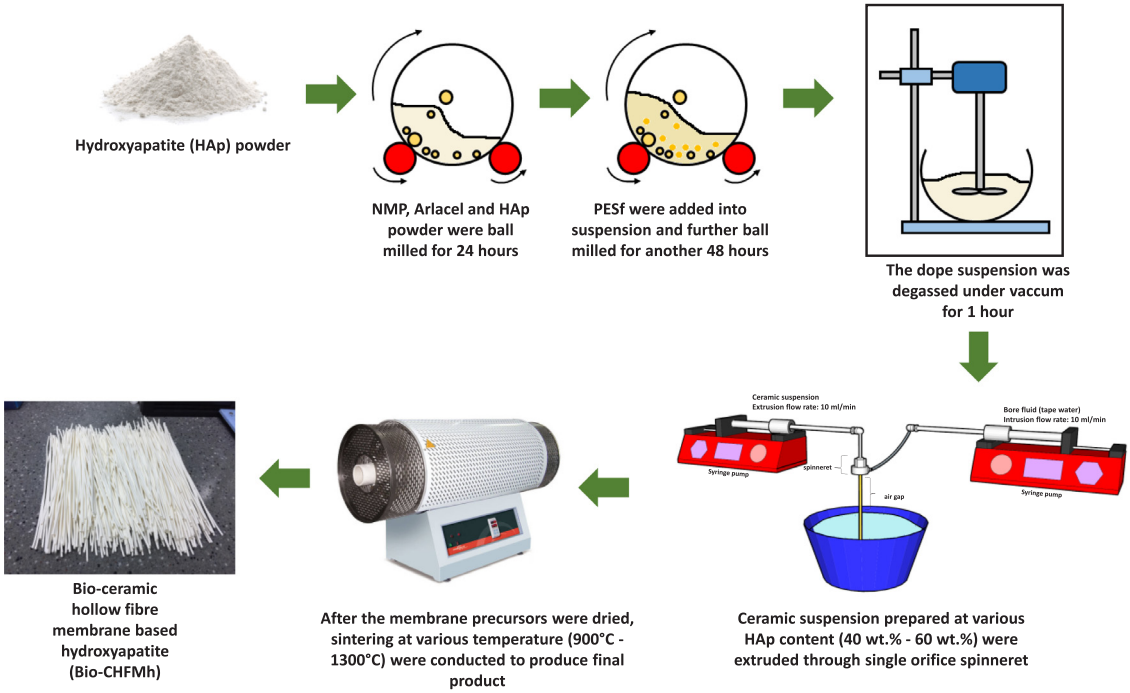

Fig. 2. Preparation of hydroxyapatite-based bio-ceramic hollow fiber membrane via phase inversion and sintering technique.

controlled by infusion pumps (Harvard Apparatus, PHD 2000 Programmable and Chemyx Inc., Model Nexus 6000) whereas the bore fluid rate was controlled using a bore pump (AB, Japan). Both suspension and bore fluid flow rates were set as 10 mL/min; the air gap distance was fixed at 5 cm. The as-prepared membrane precursors were dried overnight before cutting into the desired length. This was followed by the sintering process in which the precursors were sintered at various temperatures ranging from 900 to 1300 °C in a tubular furnace (XY-Magna 5000). Initially, the temperature was increased from room temperature to 600 °C at 2 °C /min and held for 2 h. The temperature was further increase to target temperature at 5 °C /min and held for 3 h. Finally, it was cooled down to room temperature at a rate of 5 °C /min. More details on ceramic hollow fiber membrane fabrication could be found in our previous studies [7,14,33].

2.5. Characterization of hydroxyapatite-based bio-ceramic hollow fiber membrane

The surface and cross section morphologies of the prepared h-bio-CHFMs were analyzed using SEM (TM 3000, Hitachi). The samples were coated with gold prior to the analysis. The mechanical strength of the h-bio-CHFMs was measured through three-points bending test using an Instron Model 5544 tensile tester provided with a load cell of 1 kN. The membranes were fixed on the sample holder with a 30 mm distance. The bending strength, σ_F was calculated using equation (1):

$$\sigma_F = \frac{8FLD_o}{\pi(D_o^4 - D_i^4)} \quad (1)$$

where F is the measured load at which fracture occurred (N), whereas L, D_o and D_i are the length, outer and inner diameters (m) of the membranes, respectively.

Mercury intrusion porosimeter (Micromeritics, AutoPore IV, 9500) combined with Micromeritics software (version 1.09) was used to determine the pore size distribution and overall porosity of the membranes prepared at different sintering temperatures. The surface morphology and roughness of membranes prepared at different sintering temperatures were investigated using atomic force microscopy (AFM: PARK XE-100, Schaefer Technologie GmbH). The surface roughness was obtained by tip scanning with scan size of 10 μm × 10 μm.

2.6. Performance of hydroxyapatite-based bio-ceramic hollow fiber membrane in domestic wastewater treatment

The feasibility of the prepared h-bio-CHFMs in treating industrial textile wastewater was investigated at 120 min. The wastewater was obtained from a textile mill operated by Ramatex Industries in Sri Gading, Batu Pahat, Johor, Malaysia (1.844582, 102.949816). Table 1 summarizes the characteristics of the wastewater collected. Prior to the separation test, the wastewater sample was filtered using Whatman filter paper no. 1 (11 μm) to remove the suspended solids like sand and dust. h-bio-CHFMs prepared at different sintering temperatures were used for the separation performance test. The characteristics of the wastewater, such as color (XHG, Japan), conductivity (portable conductivity meter, EC300, YSI Inc.), chemical oxygen demand (COD) (DR 5000, Hach Spectrophotometer, USA) and turbidity (2100Q, Hach Turbidemeter, USA), were measured before and after the separation process. In addition, the removal of heavy metals from the wastewater was measured using atomic adsorption spectroscopy (AAS, Aanalyst 800). The preparation also involve digestion with a concentrated acid of 0.1 M HCl. After that, dilution was made before injecting it into AAS. Herein, 5 mL dilution in 50 mL was made.

Table 1
Characteristics of the collected industrial textile wastewater.

Parameters	Value
COD	352–416 mg/L
Color	1211–1478 Pt/C_o
Turbidity	25–31 NTU
Conductivity	1094–1614 μs/cm
Copper (Cu)	1.05 mg/L
Iron (Fe)	2.36 mg/L
Zinc (Zn)	0.90 mg/L
Chromium (Cr)	1.92 mg/L
Cadmium (Cd)	0.45 mg/L

The removal coefficient, R was calculated using equation (2):

$$R(\%) = \frac{C_f - C_p}{C_f} \quad (2)$$

where C_f and C_p are the concentrations of feed and permeate, respectively.

The separation performance was conducted using a cross-flow filtration system under a pressure of 2 bar. The flux, J was determined using equation (3):

$$J = \frac{V}{A \times t} \quad (3)$$

where V is the volume of permeate collected (L), A is the surface area of the membrane (m^2) and t is the permeation time (s).

3. Results and discussion

3.1. Characteristics of the calcined cow bone

Fig. 3A and B presented the TEM images illustrating the morphology of the calcined cow bone powder which contained HAp with high purity. It was observed that the obtained HAp powders are composed of irregular crystal-like particles with an average size of 1 μm. In a recent work conducted by Pal et al. [22], the HAp derived from fish bone also demonstrated similar morphology. In addition, some distinct spots arranged in a ring-like manner was also observed as shown in Fig. 3C. This SAED pattern indicates the polycrystalline nature of the obtained HAp powder.

Fig. 4A demonstrates the XRD pattern of HAp produced through the calcination of WCB at 800 °C. The XRD spectrum was compared with the standard JCPDS (# 00-024-0033) data of pure HAp [34]. The sharp peaks present in the XRD spectrum confirmed the crystallinity of the obtained HAp powder; all these peaks were closely matched with the peaks of pure HAp. Hence, it shows that the WCB was successfully converted into HAp powder through thermal treatment. In addition, a well-resolved characteristic peak of highest intensity was obtained at the 2θ value of 31.77°, corresponding to (2 1 1) plane of pure HAp [35]. The formation of HAp from WCB through thermal treatment was further confirmed by FTIR analysis (Fig. 4B). As observed, the peaks centered at 962 cm^{-1}, 1021 cm^{-1} and 1088 cm^{-1} corresponded to the stretching vibration of P-O bonds. Meanwhile, a small peak at 874 cm^{-1} signifies the presence of carbonate. The peak with the lowest intensity centered at 3573 cm^{-1} was attributed to the stretching vibration of O–H groups. Fig. 4C demonstrates the thermogravimetric/differential (TG/DTA) analysis results of the calcined WCB. From the TG curve, it was observed that no phase transformation occurred throughout the heating. The weight loss observed was probably due to the elimination of the remaining residues in the calcined WCB. Moreover, the DTA curve also does not show any peak that indicates the phase transformation of HAp at very high temperature. It is worth to note that similar TG/DTA trend was also observed by Finisie et al. [36] who used synthetic HAp in their work.

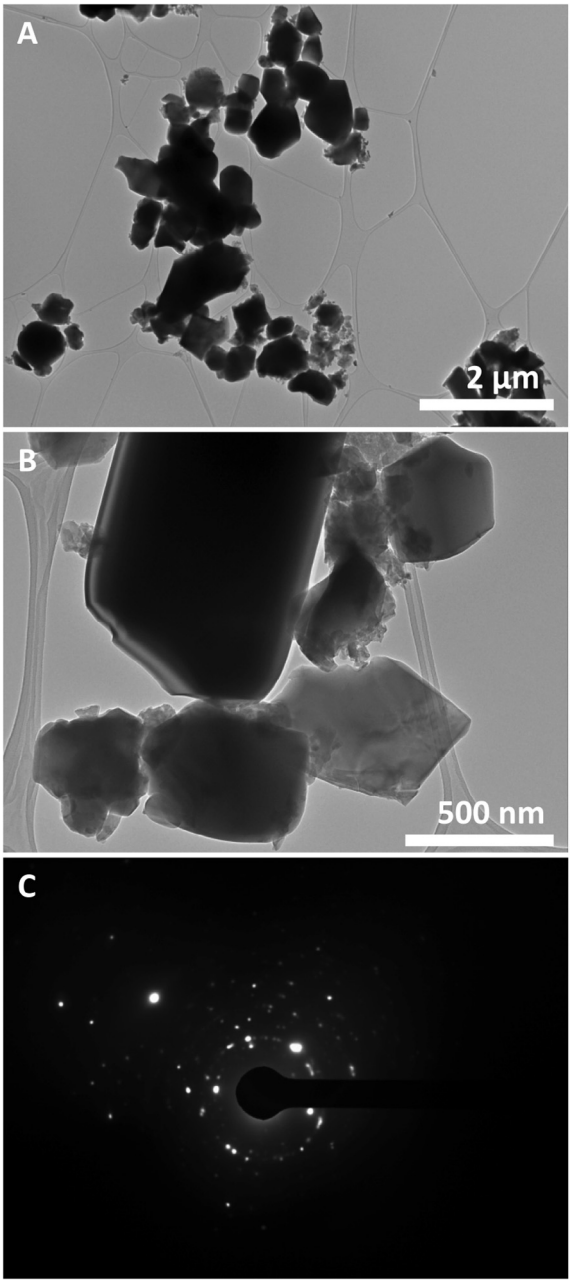

Fig. 3. TEM images of the prepared HAp: (A) overall particles, (B) higher magnification and (C) particle diffraction.

3.2. Characterization of hydroxyapatite-based bio-ceramic hollow fiber membrane

3.2.1. Effect of hydroxyapatite content

The h-bio-CHFMs were successfully prepared through phase inversion/sintering technique. Fig. 5 shows the cross-sectional structure of h-bio-CHFMs prepared with different HAp contents (40, 50 and 60 wt%) at the sintering temperature of 900 °C. It was observed that these membranes exhibited the asymmetric structures of finger-like voids and sponge layer. However, the formation of the finger-like structure in h-bio-CHFM with the lowest HAp content (40 wt%) was unstable. A close-up observation on the sponge-like structure revealed that the phase inversion was also unstable. Meanwhile, the increase of the HAp content from 40 to 50 wt% improved the formation of the finger-like structure. As observed in Fig. 5B2, the finger-like voids initiated from the inner membrane surface to approximately 50% of the membrane thickness. Further increase of HAp content to 60 wt% led to the abrupt decrease in the finger-like structure thickness to approximately 10% of the membrane thickness. Fig. 6 demonstrates the effect of HAp content on the viscosity of the ceramic suspensions. The rheological profiles of the ceramic suspensions with different HAp content decreased with an increase of shear rate from 1 to 100 s^{-1}, thus, obeying the shear thinning behavior [37]. In this work, the viscosities of the ceramic suspensions were determined at the shear rate of 50 s^{-1}. The viscosities of suspensions with HAp content of 40, 50 and 60 wt% were 840, 7050 and 9616 cP, respectively. Whereas, the viscosity for suspension containing 70 wt% of HAp content is slightly higher than other suspension. Unfortunately, due to the extremely high viscosity of the suspension, no ceramic precursor can be extruded through the spinneret as the suspension was blocked in the spinneret.

According to Kingsbury and Li [38], the finger like formation was greatly affected by the suspension viscosity. The authors found that the increasing viscosity inhibited the “viscous fingering” mechanism during the phase inversion process. Later, Wang and Lai [39] proved that this mechanism can be correlated with the concept of fluid replacement in porous media. During phase inversion of h-bio-CHFM, less viscous water that act as non-solvent replace ceramic suspension that is more viscous fluid than water through interfacial tension. In this case, uneven fronts of the non-solvent invade the ceramic suspension and form complex pattern, often taking finger-like shape. However, when the viscosity of ceramic suspension is too high, no interfacial tension occur and resulting a membrane without finger-like structure. More detail information on viscous fingering mechanism can be found elsewhere [39,40].

Another remarkable changes that can be observed is the increment of membrane thickness with increasing HAp content. From SEM image (Fig. 5), the thickness of ceramic membrane is increased from 0.15 mm to 0.23 mm when the HAp content is increased from 40 wt% to 60 wt% (supplementary information). This finding is consistent with the most previous woks on ceramic membrane that deals with ceramic content [9,41,42]. According to Jamalludin et al. [32], the increment of membrane thickness is due to insufficient bore fluid flow rate that cannot withstand a hydrodynamic force due to the high viscosity. Therefore, it can be concluded here that the viscosity threshold of this work is 9616 cP, in which prepared from 60 wt% of HAp content.

To further investigate the effect of HAp content on the membrane characteristics, the mechanical strengths of the bio-CHFMh prepared with different HAp content were determined using the three-point bending test (Fig. 7). The mechanical strength of the membranes increased with higher HAp content due to the presence of the thinner finger-like structure. The h-bio-CHFM prepared with 40 wt% of HAp content exhibited the lowest mechanical strength of 38.9 MPa. This is according to the unstable structure of the membrane as discussed in Fig. 5. Meanwhile, the h-bio-CHFM prepared with the highest HAp content of 60 wt% demonstrated the highest mechanical strength of 55.7 MPa. Herein, there are two reason can be made: (1) the size of finger-like region. According to Othman et al. [43], the finger-like structure diminished the strength of the membrane by reducing the integrity of the sponge-like structure region. The similar observation was also observed by Paiman et al. [44] who studied the yttria-stabilized zirconia. (2) thickness of the membrane. Taken together, the mechanical strengths of the membrane prepared in this study were relatively lower compared to those obtained in most of the previous studies (> 100 MPa). This can be explained by the mechanism of the neck growth between the HAp particles that failed to induce the shrinkage or densification at the low sintering temperature of 900 °C [45]. Therefore, it was necessary to study the effect of sintering temperature towards the h-bio-CHFMs.

3.2.2. Effect of sintering temperature

The effect of sintering temperature ranging from 900 to 1300 °C towards the h-bio-CHFMs was studied. h-bio-CHFM prepared with

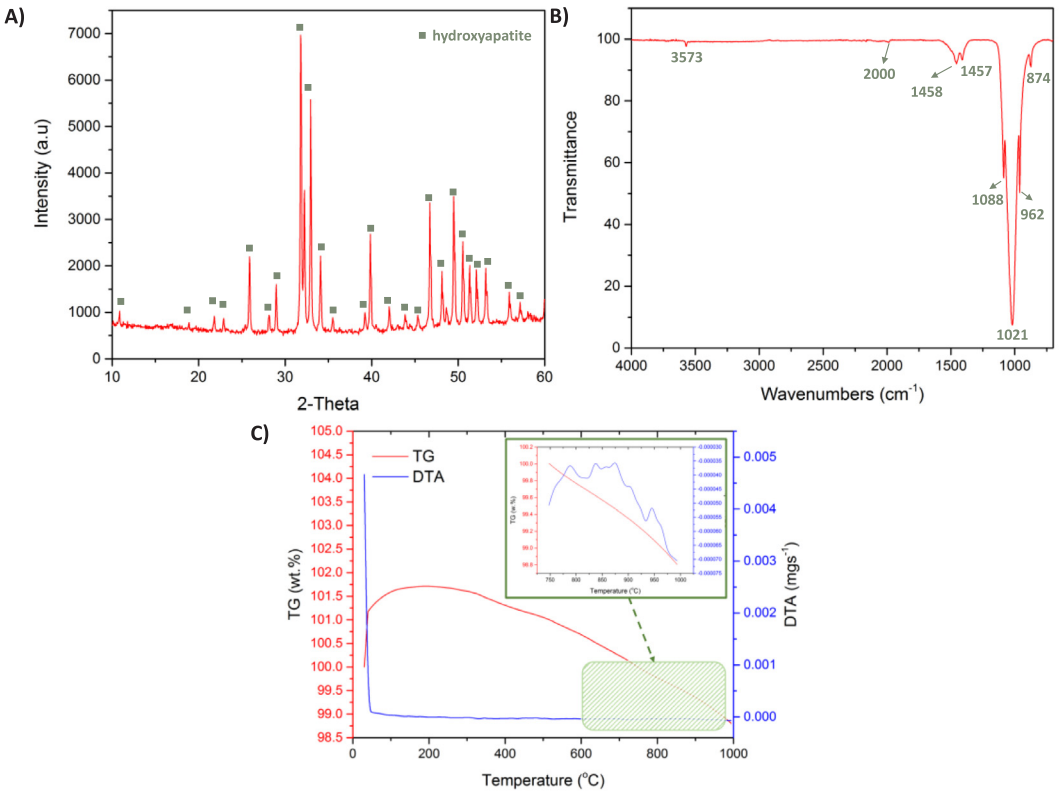

Fig. 4. (A) XRD patterns, (B) FT-IR spectra, (C) TG/DTA of the prepared HAp powders.

60 wt% HAp content was selected for this study on the effect of sintering temperature because the h-bio-CHFMs with lower HAP content were unstable. In addition, the h-bio-CHFM also exhibited the highest mechanical strength as illustrated in Fig. 7. Accordingly, the cross-sectional SEM images of the obtained h-bio-CHFMs with different sintering temperatures are shown in Fig. 8. Interestingly, the sponge-like region consists of unique cylindrical rod-shaped particles. It could be seen that the increase in sintering temperature did not give any significant effect towards the finger-like voids. In contrary, the cylindrical rod-shaped HAp particles in the sponge-like region increased in size and formed the long rod-shaped particles at the higher sintering temperature. Surprisingly, the particles seemed to grow larger in size instead of having diffusion between the particles with increasing sintering temperature. This was different from most of the previous studies which reported the more rapid particle neck growth with increasing sintering temperature [33,38,43]. A close-up observation on the surface structures of h-bio-CHFMs is illustrated in Fig. 9 and showed that h-bio-CHFMs induced non-densifying neck growth [46]. This is according to the types of neck growth that can be divided into two: (1) non-densifying neck growth and (2) densifying neck growth (Fig. 9F).

Sintering is a diffusional process that proceeds at relatively high temperatures, usually between ½ and ¾ of the melting temperature of the ceramic. Accordingly, melting point of HAp is 1670 °C. At the temperature of 900 °C, the size of cylindrical rod-shaped HAp particles was less than 1 μm. When the sintering temperature was increased from 900 to 1000 °C, the HAp particles exhibited similar shape, but the pore size of the sponge-like region decreased as a result of pore densification [47]. At the sintering temperature of 1100 °C, the HAp particles started to grow larger, and the pore densification further occurred. The growth of HAp particles in the membrane matrix was more rapid at the sintering temperature of 1200 °C, resulting in a denser sponge-like structure. According to Hongjian et al. [48], the morphologies of final bio-HAp powder relies on their fabrication methods, whether it is co-precipitation, hydrothermal or sintering method. Thangamani et al. [49] found that the crystallographic facets of the HAp powders grew rapidly during sintering, resulting in needle-like, elongated or round shapes. These particle shapes are desired by most of the researchers due to their ability to enhance the separation performance [50]. At the sintering temperature of 1300 °C, densification of the HAp particles took place, and the micro-size pinhole pores were formed on both the cross-section and surface of the h-bio-CHFM.

Membrane pore size is very important in the separation process. It plays a major role in separating the feed components with different particle size via sieving mechanism [51]. The results of the investigation on the pore size of h-bio-CHFMs with different sintering temperatures are presented in Fig. 10. The results indicate that all the membranes consist of two different pore types, namely finger-like voids and sponge-like pores. For h-bio-CHFM sintered at 900 °C, the peak at ~1.121 μm was attributed to the finger-like voids whereas the peak at 0.081 μm corresponded to the sponge-like pores. As the sintering temperature was increased to 1000 °C, pore reduction occurred by which both the peaks representing the finger-like voids and sponge-like pores were shifted to 0.871 and 0.032 μm, respectively. At the sintering temperature of 1100 °C, the cylindrical rod-shaped HAp particles started to elongate and increase in size, which further reduced the pore size. Hence, the size of the sponge-like pores decreased to 0.021 μm while no change was observed for finger-like pore size. Interestingly, the h-bio-CHFM sintered at 1200 °C possessed nano-size membrane pores in the sponge-like region with an average size of 0.013 μm (13 nm). From Figs. 8 and 9, it could be observed that the pores in the sponge-like region of the membrane were diminish due to the elongation of the rod-shaped HAp particles. Accordingly, the h-bio-CHFM sintered at 1300 °C exhibited larger sponge-like pore size of 0.3 μm compared to that of the membrane sintered at 1200 °C. It was attributed to the formation of pinhole pores in the membrane structure.

Fig. 11 shows the porosity of the h-bio-CHFMs as a function of sintering temperature. As expected, the membrane porosity decreased with increasing sintering temperature from 900 to 1200 °C and slightly

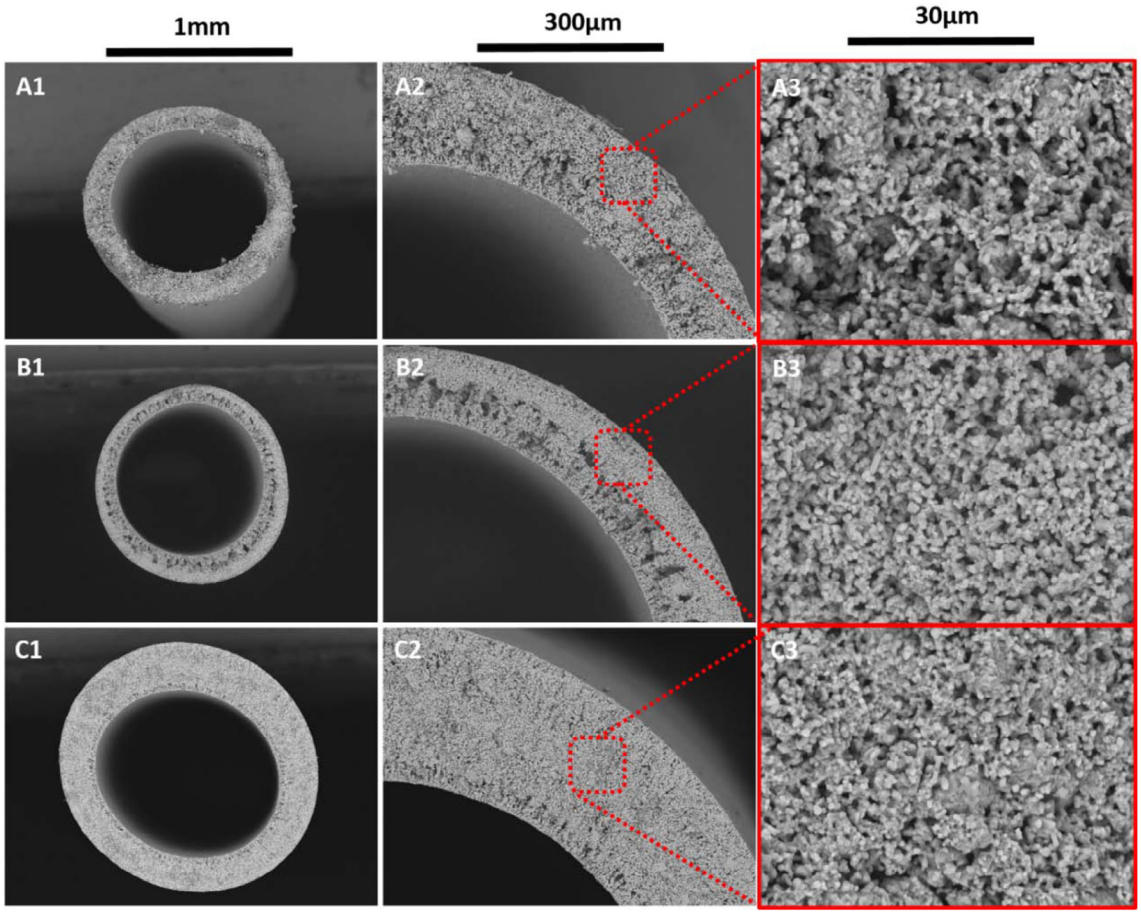

Fig. 5. Cross-sectional SEM images of the h-bio-CHFMs prepared with different HAp content at the sintering temperature of 900 °C: (A) 40 wt%, (B) 50 wt% and (C) 60 wt%; (1) the overall cross section, (2) finger-like structure, and (3) sponge-like structure at higher magnification.

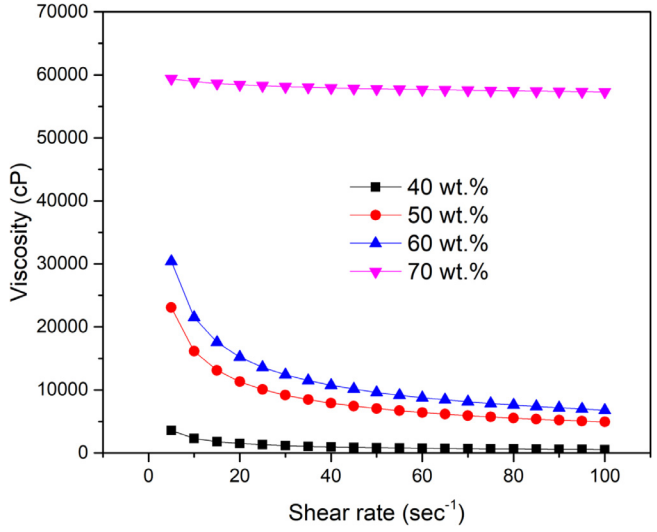

Fig. 6. Viscosity of the ceramic suspension with different HAp content.

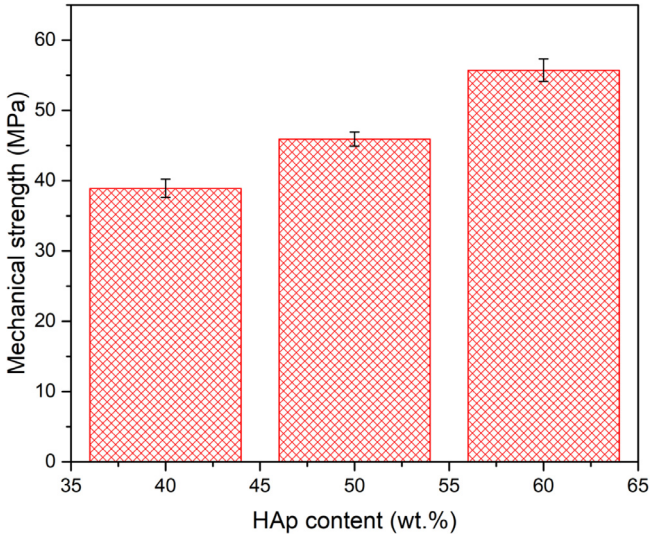

Fig. 7. Mechanical strength of h-bio-CHFMs prepared with different HAp content at the sintering temperature of 900 °C.

increased after sintered at 1300 °C. The h-bio-CHFM sintered at 900 °C exhibited the highest porosity of 51.3%. The porosity decreased to 35.1% after sintering at 1200 °C. The h-bio-CHFM sintered at 1300 °C experienced a slight increase in porosity to 37.2% due to the presence of pinhole pores. Similar porosity trend was also reported in most of the literature on ceramic membranes [7,33,37].

As commonly known, the low mechanical strength of the ceramic membrane is one of the main constraints that need to be overcome with for large scale applications. Fig. 12 demonstrates the mechanical strengths of h-bio-CHFMs sintered at different temperatures. The mechanical strength of the membranes increased with the increasing sintering temperature as a result of the elongation of cylindrical rod-shaped HAp particles in the membrane matrix. The elongation of HAp particles increased the integrity of the sponge-like structure region,

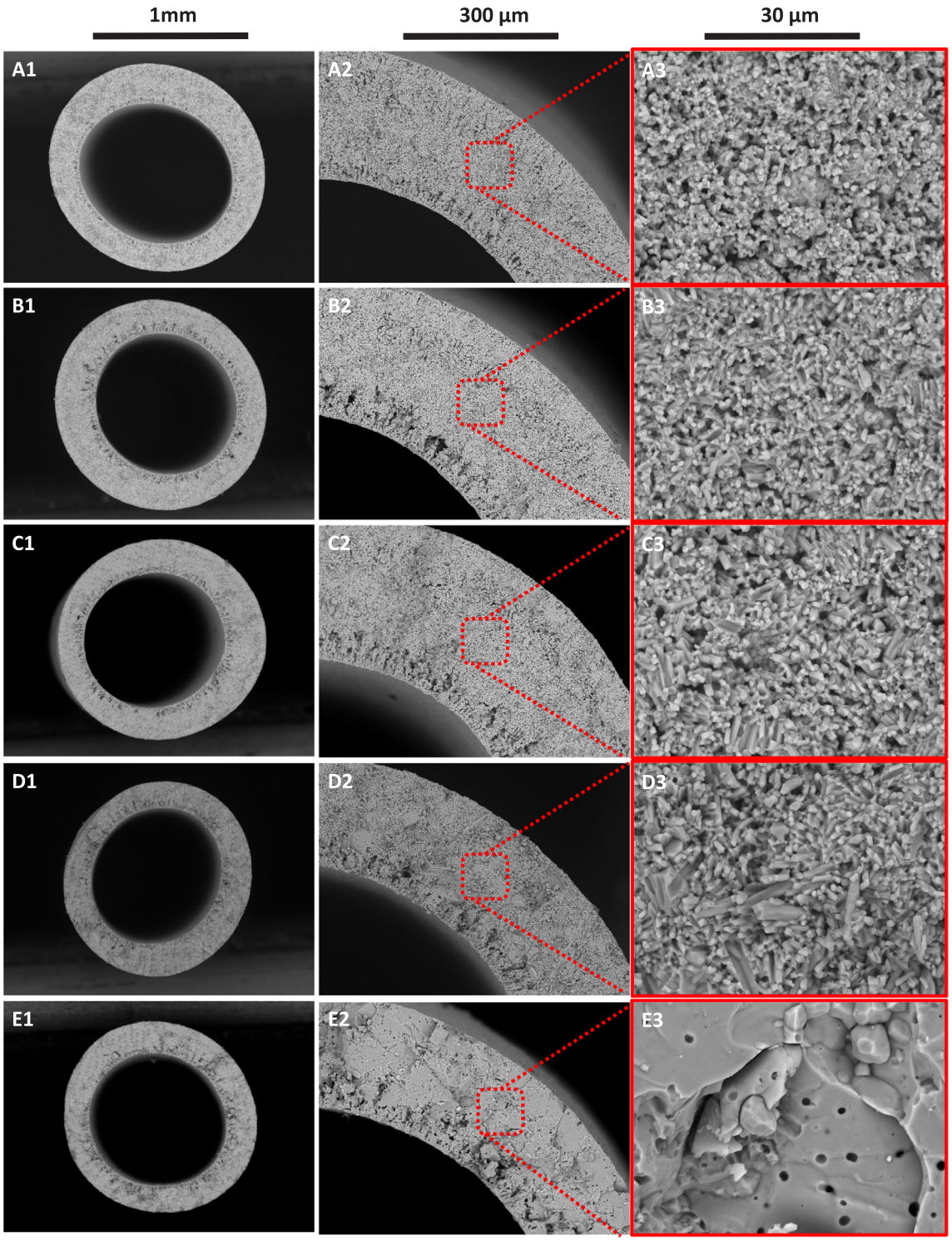

Fig. 8. Cross-sectional SEM images of h-bio-CHFMs prepared with 60 wt% HAp content at different sintering temperatures: (A) 900 °C, (B) 1000 °C, (C) 1100 °C, (D) 1200 °C, and (E) 1300 °C; (1) overall cross section, (2) finger-like structure, and (3) sponge-like structure at high magnification.

thus, improving the mechanical strength of the membrane. As expected, the h-bio-CHFM sintered at 900 °C exhibited the lowest mechanical strength of 53.2 MPa. On the other hand, the h-bio-CHFM sintered at 1200 °C had the longest cylindrical rod-shaped HAp particles which bestowed it with the highest mechanical strength (202.5 MPa). The mechanical strength of h-bio-CHFM significantly decreased to 98.3 MPa when the sintering temperature was further increased to 1300 °C. It was due to the formation of micron size pinhole pores (1–2 µm) during the HAp particle densification process as shown in Figs. 8 and 9. According to Rice [52], pinhole pores induced low porosity (Fig. 11) and were considered as the membrane defects that reduced the mechanical strength of the membrane. Remarkably, the mechanical strength of the h-bio-CHFM was comparable with that of the alumina membranes (50–250 MPa) [53,54].

3.3. Performance of bio-ceramic hollow fiber membranes

The performance of the h-bio-CHFMs sintered at different

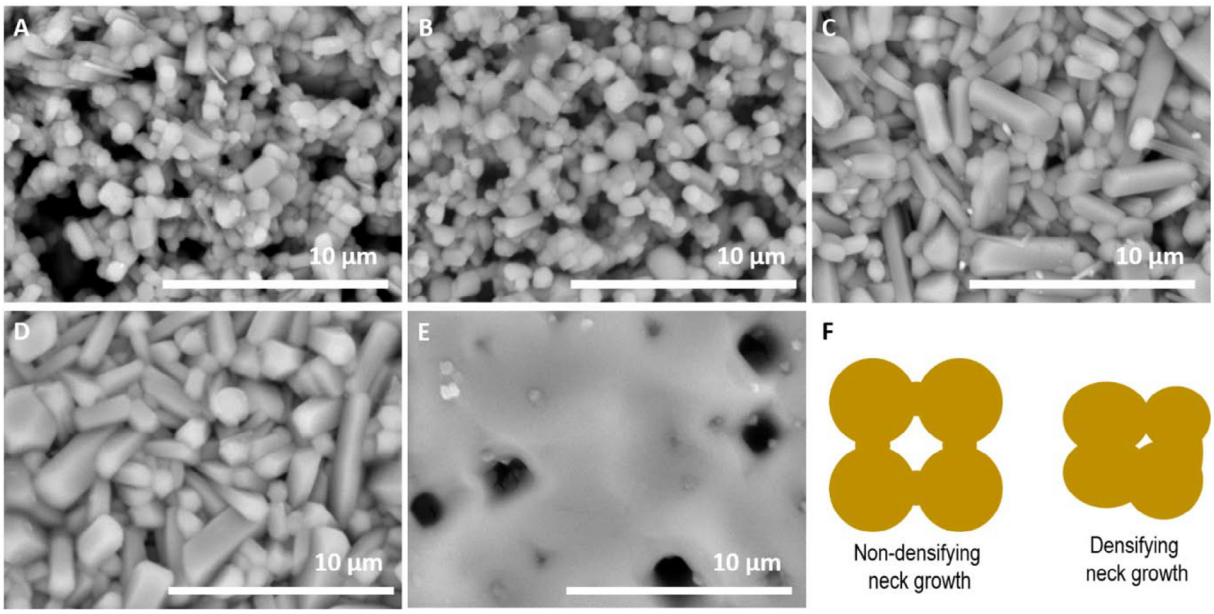

Fig. 9. Surface SEM images of h-bio-CHFMs prepared with 60 wt% HAp content at different sintering temperatures: (A) 900 °C, (B) 1000 °C, (C) 1100 °C, (D) 1200 °C, and (E) 1300 °C.

temperatures in treating the industrial textile wastewater was investigated. Membrane flux is an important membrane operating parameter and defined as the permeate flow divided by the total membrane surface area at required time, as presented in Fig. 13. Fig. 13 illustrates the permeate flux variations of the h-bio-CHFMs throughout the 120-minutes performance test. It could be seen that the flux decreased for the membranes with higher sintering temperatures. Accordingly, the h-bio-CHFM sintered at 1000 °C experienced a rapid decline in the initial flux (180.8 L/m^{2}h) compared to that of h-bio-CHFM sintered at 900 °C (210.5 L/m^{2}h). The fluxes became stable at t = 40 min with the values of 121.7 and 105.4 L/m^{2}h for the h-bio-CHFMs sintered at 900 and 1000 °C, respectively. Similar findings were also reported in the literature [55–57]. According to Dilaver et al. [58], the flux decline rate relied on the membrane pore size and wastewater type; the membranes with larger pore size experienced more rapid flux decline due to the membrane fouling mechanism. Hence, further study on the fouling of the h-bio-CHFM will be conducted. For the h-bio-CHFM sintered at 1100 °C, the flux became stable earlier at t = 25 min with the value of 94.8 L/m^{2}h compared to those membranes sintered at lower temperatures. Interestingly, a stable flux of 88.3 L/m^{2}h was observed at t = 0 min for the h-bio-CHFM sintered at 1200 °C which exhibited the smallest pore size. In addition, no flux was obtained for the h-bio-CHFM sintered at 1300 °C due to the formation of pinhole pores in the membrane structure. According to Gitis and Rothenberg [59], the pinhole

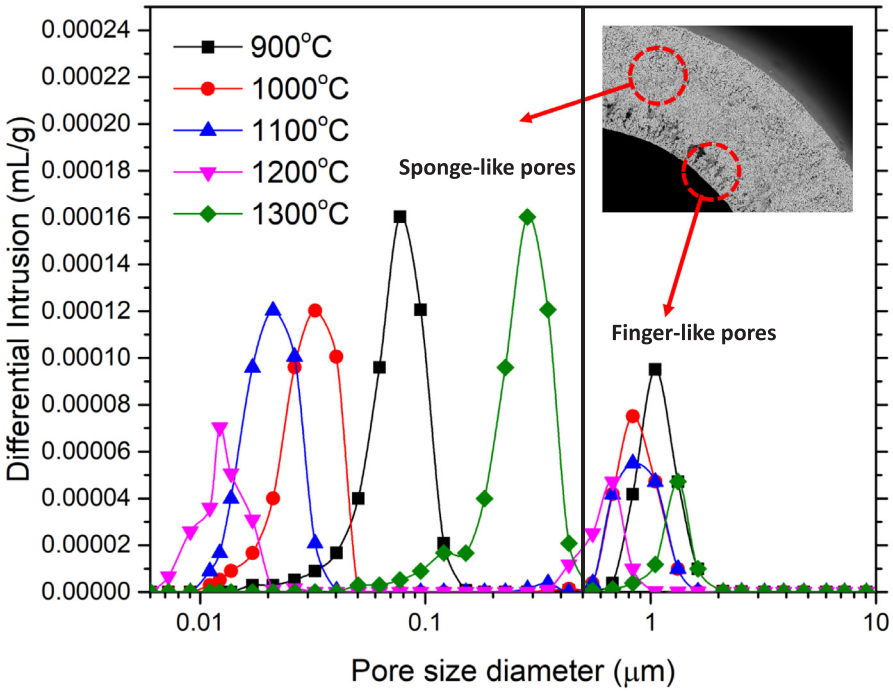

Fig. 10. Pore size distribution of the h-bio-CHFMs with 60 wt% HAp content at different sintering temperatures.

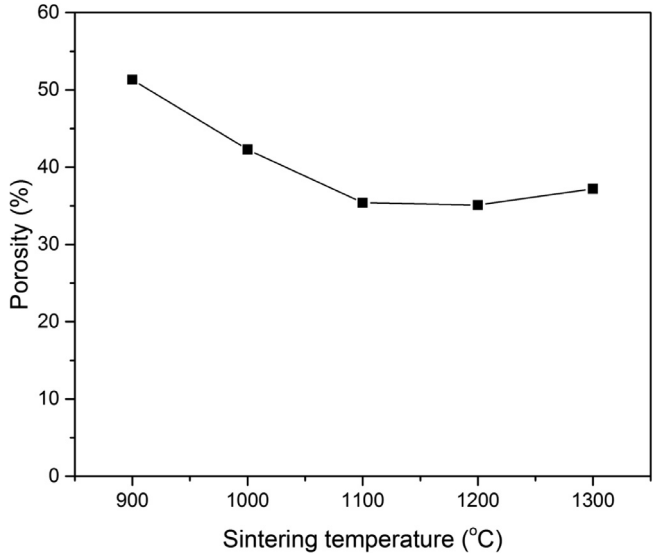

Fig. 11. Porosity of the h-bio-CHFMs prepared with 60 wt% HAp content at different sintering temperatures.

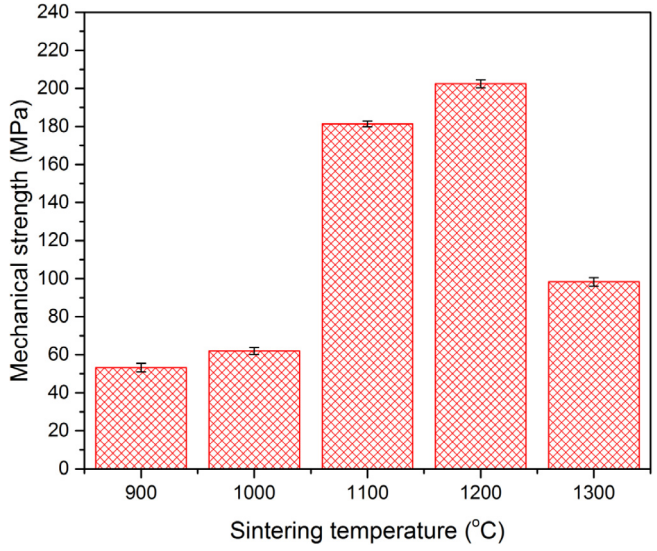

Fig. 12. Mechanical strength of the h-bio-CHFMs prepared with 60 wt% HAp content at different sintering temperatures.

pores do not contribute to the membrane porosity and liquid flow across the membrane; these pores are dead-end and have incomplete pore path. Hence, it is concluded that the optimum sintering temperature for the h-bio-CHFM was 1200 °C in which the membrane exhibited high mechanical strength and flux performance. Interestingly, the flux of this result is comparable to polymeric membrane (2–6 L/m^{2}h) [60].

The characteristics of the permeate was investigated and presented in Table 2. H-bio-CHFM sintered at 1200 °C showed the excellent performance in treating industrial textile wastewater with the highest removal efficiency of 80.1, 99.9, 99.4 and 30.1% for the COD, color, turbidity and conductivity, respectively. The removal performance of the h-bio-CHFM sintered at 1300 °C could not be determined because no flux was obtained throughout the testing period (Fig. 13). The results obtained in this study were in agreement with the outcomes reported in the previous studies in which the removal efficiency was the highest for the ceramic membrane with the smallest pore size [58]. In addition, the h-bio-CHFMs also demonstrated high adsorption ability with excellent heavy metal removal performance. All the h-bio-CHFMs sintered at

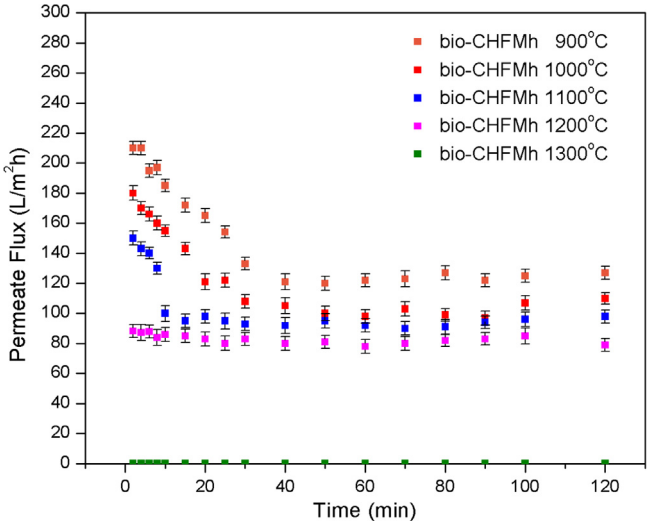

Fig. 13. Variations in the permeate flux of the h-bio-CHFMs prepared at various sintering temperature.

Table 2
Performance of the h-bio-CHFMs with different sintering temperature on the industrial textile wastewater treatment.

Removal efficiency (%)	h-bio-CHFMs with different sintering temperatures (°C)				
	900	1000	1100	1200	1300
COD	14.5	15.1	68.9	80.1	N/A
Color	27.8	44.1	85.3	99.9	N/A
Turbidity	43.2	46.9	91.3	99.4	N/A
Conductivity	6.3	7.8	26.5	30.1	N/A
Copper (Cu)	98.2	~100	~100	~100	N/A
Iron (Fe)	99.3	~100	~100	~100	N/A
Zinc (Zn)	98.5	~100	~100	~100	N/A
Chromium (Cr)	98.9	~100	~100	~100	N/A
Cadmium (Cd)	99.6	~100	~100	~100	N/A

1000 to 1200 °C had 100% removal on Cu, Fe, Zn, Cr and Cd. Two separation mechanisms might be involved during the process, namely, (1) sieving mechanism which was affected by the membrane pore size, and (2) adsorption mechanism in which the separation performance was determined by the electronegativity and adsorption ability of the membrane [5]. Based on the literature, the HAp powder exhibited a strong negative charge at the pH of 4 to 12 [61]. The pH of the wastewater used in this study was 7.3. Hence, the positively-charged heavy metal ions in the wastewater showed strong adsorption affinity towards the highly negatively charged h-bio-CHFMs, resulting in high heavy metal removal performance. Further study on the adsorption mechanism of the h-bio-CHFMs will be studied in future.

Today, the use of HAp for heavy metal adsorption has received worldwide attention. According to Choi and Jeong [62], the HAp exhibits an excellent ion-exchange ability and has been used as an agent for wastewater treatment to remove heavy metals. However, the standalone adsorption process shows some drawbacks especially it requires the additional process to remove the adsorbent from the treated wastewater. The development of HAp-based ceramic membrane with coupled adsorption and filtration abilities could overcome the problems and costs related to the adsorbent removal process. For the first time, this work successfully developed the HAp-based ceramic membrane for efficient industrial textile wastewater treatment application. The photographic image of the feed and permeate treated using h-bio-CHFMs sintered at various temperatures can be observed in Fig. S2.

4. Conclusion

In this study, HAp-based bio-ceramic hollow fiber membranes were successfully developed for industrial textile wastewater treatment. The HAp powder was synthesized from the WCB using a simple thermal method. The h-bio-CHFM prepared with 60 wt% HAp content at the sintering temperature of 1200 °C demonstrated the highest mechanical strength of 202.5 MPa with the porosity and average pore size of 35.4% and 0.013 μm, respectively. The membrane showed its huge potential for industrial textile wastewater treatment with a stable flux of 88.3 L/m^2h and excellent removal performance (color = 99.9%, COD = 80.1%, turbidity = 99.4%, conductivity = 30.1%, and heavy metals (Cu, Fe, Zn, Cr and Cd) = 100%). Currently, the fouling mechanism of the h-bio-CHFMs is being studied in our lab. Besides, the investigations on the membrane adsorption mechanism and membrane stability will also be conducted for future development of the h-bio-CHFMs.

Acknowledgement

The authors gratefully acknowledge the financial support from the Ministry of Education Malaysia under the Higher Institution Centre of Excellence Scheme (Project Number: R.J090301.7846.4J192) and Fundamental Research Grant Scheme (Project Number: 1600-RMI/ST/FRGS 5/3 (13/2016)), and also Universiti Teknologi Malaysia under the Transdisciplinary Research Grant (Project number: Q.J130000.3509.05G75), Malaysia Research University Network (MRUN) Grant (Project number: R.J130000.7809.4L867), UTM Fund (Project number: R.J130000.7746.4J309).

Appendix A. Supplementary data

Supplementary data to this article can be found online at https://doi.org/10.1016/j.cej.2019.122396.

References

[1] K. Paździor, L. Bilińska, S. Ledakowicz, A review of the existing and emerging technologies in the combination of AOPs and biological processes in industrial textile wastewater treatment, Chem. Eng. J. (2018).
[2] M.L. Mathew, A. Gopalakrishnan, C.T. Aravindakumar, U.K. Aravind, Low – cost multilayered green fiber for the treatment of textile industry waste water, J. Hazard. Mater. 365 (2019) 297–305.
[3] Y.C. Xu, Z.X. Wang, X.Q. Cheng, Y.C. Xiao, L. Shao, Positively charged nanofiltration membranes via economically mussel-substance-simulated co-deposition for textile wastewater treatment, Chem. Eng. J. 303 (2016) 555–564.
[4] S.K. Hubadillah, M.H.D. Othman, A.F. Ismail, M.A. Rahman, J. Jaafar, Y. Iwamoto, S. Honda, M.I.H.M. Dzahir, M.Z.M. Yusop, Fabrication of low cost, green silica based ceramic hollow fibre membrane prepared from waste rice husk for water filtration application, Ceram. Int. 44 (2018) 10498–10509.
[5] G. Zeng, Z. Ye, Y. He, X. Yang, J. Ma, H. Shi, Z. Feng, Application of dopamine-modified halloysite nanotubes/PVDF blend membranes for direct dyes removal from wastewater, Chem. Eng. J. 323 (2017) 572–583.
[6] T. Arumugham, N.J. Kaleekkal, D. Rana, Fabrication of novel aromatic amine functionalized nanofiltration (NF) membranes and testing its dye removal and desalting ability, Polym. Test. 72 (2018) 1–10.
[7] S.K. Hubadillah, M.H.D. Othman, Z. Harun, A.F. Ismail, M.A. Rahman, J. Jaafar, S.M. Jamil, N.H. Mohtor, Superhydrophilic, low cost kaolin-based hollow fibre membranes for efficient oily-wastewater separation, Mater. Lett. 191 (2017) 119–122.
[8] S.K. Hubadillah, Z. Harun, M.H.D. Othman, A.F. Ismail, W.N.W. Salleh, H. Basri, M.Z. Yunos, P. Gani, Preparation and characterization of low cost porous ceramic membrane support from kaolin using phase inversion/sintering technique for gas separation: Effect of kaolin content and non-solvent coagulant bath, Chem. Eng. Res. Des. 112 (2016) 24–35.
[9] Z. Harun, S. Hubadillah, S. Hasan, M.Z. Yunos, Effect of thermodynamic properties on porosity of ceramic membrane prepared by phase inversion, Appl. Mech. Mater. 575 (2014) 31–35.
[10] B. Alfiyan, H. Susanto, Utilization of fly ash as ceramic support mixture for the synthesis of zeolite pervaporation membrane, Adv. Mater. Res. 896 (2014) 74–77.
[11] Y.M. Jo, R. Huchison, J.A. Raper, Preparation of ceramic membrane filters, from waste fly ash, suitable for hot gas cleaning, Waste Manage. Res. 14 (1996) 281–295.
[12] J. Fang, G. Qin, W. Wei, X. Zhao, L. Jiang, Elaboration of new ceramic membrane from spherical fly ash for microfiltration of rigid particle suspension and oil-in-water emulsion, Desalination 311 (2013) 113–126.
[13] Q. Lü, X. Dong, Z. Zhu, Y. Dong, Environment-oriented low-cost porous mullite ceramic membrane supports fabricated from coal gangue and bauxite, J. Hazard. Mater. 273 (2014) 136–145.
[14] S.K. Hubadillah, M.H.D. Othman, Z. Harun, A.F. Ismail, M.A. Rahman, J. Jaafar, A novel green ceramic hollow fiber membrane (CHFM) derived from rice husk ash as combined adsorbent-separator for efficient heavy metals removal, Ceram. Int. 43 (2017) 4716–4720.
[15] K.M.N. Islam, Municipal solid waste to energy generation in bangladesh: possible scenarios to generate renewable electricity in Dhaka and Chittagong city, J. Renewable Energy 2016 (2016) 16.
[16] D. Hoornweg, P. Bhada-Tata, What a Waste : A Global Review of Solid Waste, Management. In: The World Bank (2012).
[17] A. Periathamby, F.S. Hamid, K. Khidzir, Evolution of solid waste management in Malaysia: impacts and implications of the solid waste bill, J. Mater. Cycles Waste Manage. 11 (2009) (2007) 96–103.
[18] W. Zheng, K. Phoungthong, F. Lü, L.-M. Shao, P.-J. He, Evaluation of a classification method for biodegradable solid wastes using anaerobic degradation parameters, Waste Manage. 33 (2013) 2632–2640.
[19] A.A. Kadir, M.S.A.M. Sani, Solid waste composition study at Taman Universiti, Parit Raja, Batu Pahat, IOP Conf. Ser.: Mater. Sci. Eng. 136 (2016) 012048.
[20] K. Shahzad, A.S. Nizami, M. Sagir, M. Rehan, S. Maier, M.Z. Khan, O.K.M. Ouda, I.M.I. Ismail, A.O. BaFail, Biodiesel production potential from fat fraction of municipal waste in Makkah, PLoS ONE 12 (2017) e0171297.
[21] B.R. Sunil, M. Jagannatham, Producing hydroxyapatite from fish bones by heat treatment, Mater. Lett. 185 (2016) 411–414.
[22] A. Pal, S. Paul, A.R. Choudhury, V.K. Balla, M. Das, A. Sinha, Synthesis of hydroxyapatite from Lates calcarifer fish bone for biomedical applications, Mater. Lett. 203 (2017) 89–92.
[23] U. Iriarte-Velasco, J.L. Ayastuy, Z. Boukha, R. Bravo, M.Á. Gutierrez-Ortiz, Transition metals supported on bone-derived hydroxyapatite as potential catalysts for the Water-Gas Shift reaction, Renewable Energy (2017).
[24] M.H. Santos, M.d. Oliveira, L.P.d.F. Souza, H.S. Mansur, W.L. Vasconcelos, Synthesis control and characterization of hydroxyapatite prepared by wet precipitation process, Mater. Res. 7 (2004) 625–630.
[25] N.A.M. Barakat, M.S. Khil, A.M. Omran, F.A. Sheikh, H.Y. Kim, Extraction of pure natural hydroxyapatite from the bovine bones bio waste by three different methods, J. Mater. Process. Technol. 209 (2009) 3408–3415.
[26] A.N.K. Ahmad Fara, M.A. Yahya, H.Z. Abdullah, Preparation and characterization of biological hydroxyapatite (hap) obtained from tilapia fish bone, Adv. Mater. Res. 1087 (2015) 152–156.
[27] W. Lemlikchi, P. Sharrock, M.O. Mecherri, M. Fiallo, A. Nzihou, Treatment of textile waste waters by hydroxyapatite co-precipitation with adsorbent regeneration and reuse, Waste Biomass Valorization 3 (2012) 75–79.
[28] J.C. Moreno, R. Gómez, L. Giraldo, Removal of Mn, Fe, Ni and Cu Ions from wastewater using cow bone charcoal, Materials 3 (2010) 452–466.
[29] R. Slimani, I. El Ouahabi, A. Elmchaouri, B. Cagnon, S. El Antri, S. Lazar, Adsorption of copper (II) and zinc (II) onto calcined animal bone meal: Part I: Kinetic and thermodynamic parameters, Chem. Data Collections 9 (2017) 184–196.
[30] M.N. Hassan, M.M. Mahmoud, A.A. El-Fattah, S. Kandil, Microwave-assisted preparation of Nano-hydroxyapatite for bone substitutes, Ceram. Int. 42 (2016) 3725–3744.
[31] S.K. Hubadillah, M.H.D. Othman, T. Matsuura, M.A. Rahman, J. Jaafar, A.F. Ismail, S.Z.M. Amin, Green silica-based ceramic hollow fiber membrane for seawater desalination via direct contact membrane distillation, Sep. Purif. Technol. 205 (2018) 22–31.
[32] M.R. Jamalludin, Z. Harun, M.H.D. Othman, S.K. Hubadillah, M.Z. Yunos, A.F. Ismail, Morphology and property study of green ceramic hollow fiber membrane derived from waste sugarcane bagasse ash (WSBA), Ceram. Int. 44 (2018) 18450–18461.
[33] S.K. Hubadillah, M.H.D. Othman, Z. Harun, A.F. Ismail, Y. Iwamoto, S. Honda, M.A. Rahman, J. Jaafar, P. Gani, M.N. Mohd, Sokri, Effect of fabrication parameters on physical properties of metakaolin-based ceramic hollow fibre membrane (CHFM), Ceram. Int. 42 (2016) 15547–15558.
[34] S. Mondal, U. Pal, A. Dey, Natural origin hydroxyapatite scaffold as potential bone tissue engineering substitute, Ceram. Int. 42 (2016) 18338–18346.
[35] S. Mondal, S. Mahata, S. Kundu, B. Mondal, Processing of natural resourced hydroxyapatite ceramics from fish scale, Adv. Appl. Ceram. 109 (2010) 234–239.
[36] M.R. Finisie, A. JosuÉ, V.T. FÁVere, M.C.M. Laranjeira, Synthesis of calcium-phosphate and chitosan bioceramics for bone regeneration, Anais da Academia Brasileira de Ciências 73 (2001) 525–532.
[37] B.F.K. Kingsbury, Z. Wu, K. Li, A morphological study of ceramic hollow fibre membranes: A perspective on multifunctional catalytic membrane reactors, Catal. Today 156 (2010) 306–315.
[38] B.F.K. Kingsbury, K. Li, A morphological study of ceramic hollow fibre membranes, J. Membr. Sci. 328 (2009) 134–140.
[39] B. Wang, Z. Lai, Finger-like voids induced by viscous fingering during phase inversion of alumina/PES/NMP suspensions, J. Membr. Sci. 405–406 (2012) 275–283.
[40] G.M. Homsy, Viscous fingering in porous media, Annu. Rev. Fluid Mech. 19 (1987) 271–311.
[41] S.K. Hubadillah, M.H.D. Othman, M.A. Rahman, A.F. Ismail, J. Jaafar, Preparation and characterization of inexpensive kaolin hollow fibre membrane (KHFM) prepared using phase inversion/sintering technique for the efficient separation of real oily wastewater, Arabian J. Chem. (2018).
[42] S.K. Hubadillah, P. Kumar, M.H. Dzarfan Othman, A.F. Ismail, M.A. Rahman,

J. Jaafar, A low cost, superhydrophobic and superoleophilic hybrid kaolin-based hollow fibre membrane (KHFM) for efficient adsorption-separation of oil removal from water, RSC Adv. 8 (2018) 2986–2995.
[43] M.H.D. Othman, Z. Wu, N. Droushiotis, G. Kelsall, K. Li, Morphological studies of macrostructure of Ni–CGO anode hollow fibres for intermediate temperature solid oxide fuel cells, J. Membr. Sci. 360 (2010) 410–417.
[44] S.H. Paiman, M.A. Rahman, M.H.D. Othman, A.F. Ismail, J. Jaafar, A.A. Aziz, Morphological study of yttria-stabilized zirconia hollow fibre membrane prepared using phase inversion/sintering technique, Ceram. Int. 41 (2015) 12543–12553.
[45] R.M. German, 1 - Thermodynamics of sintering A2 - Fang, Zhigang Zak, Sintering of Advanced Materials, Woodhead Publishing, 2010, pp. 3–32.
[46] P. Šajgalík, M. Haviar, Z. Pánek, Estimation of contribution of non-densifying mechanisms during sintering, Ceram. Int. 14 (1988) 63–69.
[47] K. Darcovich, F.N. Toll, A. Meurk, Sintering effects on the porous characteristics of functionally gradient ceramic membrane structures, J. Porous Mater. 8 (2001) 201–210.
[48] H. Zhou, J. Lee, Nanoscale hydroxyapatite particles for bone tissue engineering, Acta Biomater. 7 (2011) 2769–2781.
[49] N. Thangamani, K. Chinnakali, F.D. Gnanam, The effect of powder processing on densification, microstructure and mechanical properties of hydroxyapatite, Ceram. Int. 28 (2002) 355–362.
[50] B. Kowalczyk, I. Lagzi, B.A. Grzybowski, Nanoseparations: Strategies for size and/or shape-selective purification of nanoparticles, Curr. Opin. Colloid Interface Sci. 16 (2011) 135–148.
[51] A. Basile, A. Cassano, N.K. Rastogi, Advances in Membrane Technologies for Water Treatment: Materials, Processes and Applications, Elsevier Science, 2015.
[52] R.W. Rice, Porosity of Ceramics: Properties and Applications, Taylor & Francis, 1998.
[53] L. García-Fernández, B. Wang, M.C. García-Payo, K. Li, M. Khayet, Morphological design of alumina hollow fiber membranes for desalination by air gap membrane distillation, Desalination 420 (2017) 226–240.
[54] S. Koonaphapdeelert, K. Li, Preparation and characterization of hydrophobic ceramic hollow fibre membrane, J. Membr. Sci. 291 (2007) 70–76.
[55] R.S. Hebbar, A.M. Isloor, A.F. Ismail, Preparation and evaluation of heavy metal rejection properties of polyetherimide/porous activated bentonite clay nano-composite membrane, RSC Adv. 4 (2014) 47240–47248.
[56] A. Mansourizadeh, A. Javadi Azad, Preparation of blend polyethersulfone/cellulose acetate/polyethylene glycol asymmetric membranes for oil–water separation, J. Polym. Res. 21 (2014) 375.
[57] M. Asaadi, D.A. White, A model for determining the steady state flux of inorganic microfiltration membranes, Chemi. Eng. J. 48 (1992) 11–16.
[58] M. Dilaver, S.M. Hocaoğlu, G. Soydemir, M. Dursun, B. Keskinler, İ. Koyuncu, M. Ağtaş, Hot wastewater recovery by using ceramic membrane ultrafiltration and its reusability in textile industry, J. Cleaner Prod. 171 (2018) 220–233.
[59] V. Gitis, G. Rothenberg, Ceramic Membranes: New Opportunities and Practical Applications, Wiley, 2016.
[60] F. Galiano, I. Friha, S.A. Deowan, J. Hoinkis, Y. Xiaoyun, D. Johnson, R. Mancuso, N. Hilal, B. Gabriele, S. Sayadi, A. Figoli, Novel low-fouling membranes from lab to pilot application in textile wastewater treatment, J. Colloid Interface Sci. 515 (2018) 208–220.
[61] M. Okada, T. Matsumoto, Synthesis and modification of apatite nanoparticles for use in dental and medical applications, Jpn. Dental Sci. Rev. 51 (2015) 85–95.
[62] S. Choi, Y. Jeong, The removal of heavy metals in aqueous solution by hydroxyapatite/cellulose composite, Fibers Polym. 9 (2008) 267–270.